EASR

Engineering and Applied Science Research

https://www.tci-thaijo.org/index.php/easr/index

Published by the Faculty of Engineering, Khon Kaen University, Thailand

The combined effect of bonding and particle size variables on the undrained behavior of sandy soil

Richard Vall Ngangu Ricardo* and Musaffa Ayşen Lav

Department of Civil Engineering, Geotechnical and Soil Mechanics program, Istanbul Technical University, Maslak, 34467 Sarıyer/Istanbul, Turkey

Received 7 September 2021
Revised 17 November 2021
Accepted 19 November 2021

Abstract

Naturally bonded sands are of various gradings and behave differently from unbonded sandy soils. An understanding of the combined effect of bonding and the variation of particle size on their engineering behavior and mechanical properties is required for a better geotechnical design. In this study, the coupled influence of bonding and particle size of sand-kaolin soil mixtures was studied under different confining pressures in triaxial consolidated undrained conditions. From the results it was found that for bonded samples, the peak strength and cohesion intercept vary in the same way as the mean particle size and coefficient of uniformity, while the trend was altered for unbonded materials. However, the angle of internal friction increases in the presence of bonding and decreases as the mean particle size increases under both states. The said coupled influence was found to be more pronounced at low confining stress. The bonded soil of bigger particle size is less ductile than that of smaller particle size, particularly for the test conducted at low confining pressure.

Keywords: Particle size, Bond, Gradation, Triaxial, Sand, Cemented sands

1. Introduction

Weakly cemented sands are widely used in geotechnical engineering works. Cementation can be natural or artificial. In the natural environment, cementation results from processes such as physical and/or chemical weathering, bonding by silt or clay particles, or welding effects. Artificial cementation involves many methods through injection, grouting, mixing, or thermal process. In either case, cementation is known to improve the shear characteristic of soil.

To study the engineering behavior of bonded soils, tests are conducted in-situ or in laboratory conditions. Due to the cost and technical requirements of the in-situ tests, laboratory tests are a good alternative. The triaxial tests, among others, are one of the most used for this purpose [1-5]. From the studies of the bonded materials conducted in the triaxial equipment under undrained conditions, it is reported that their behavior and mechanical properties are governed by several parameters such as confining pressure, void ratio index, cementation degree, previous deformation history, grain size, gradation, and stress path [6-10]. Among these parameters, the influence of particle size and gradation on the behavior of sandy soils are of particular interest when using bonded sand.

Among researchers who have studied the role of particle size and gradation, Thevanayagam et al. [11] and Karimian and Hassanlourad [10] reported that the increase in mean particle size (D_{50}) due to the fine content (with FC $< 25\%$) under an undrained triaxial test results in the loss of shear strength. Belkhatir et al. [12] analyzed the behavior of uncemented sand-silt mixture specimens, of various FC under undrained triaxial conditions, and concluded that the peak strength increases together with D_{50}, while the coefficient of uniformity Cu decreases. By increasing FC, the effective diameter D_{10} declines more than D_{60} and enables Cu to rise. However, for the same amount of FC, D_{10} remains constant and the only parameter which governs Cu is D_{60}, thus in this case Cu and D_{50} are found to vary in the same direction. Another study examining the influence of the soil gradation of different fine content was done by [13]. From this experiment, Cu and D_{50} was observed to increase together, whereas the peak strength decreased.

To isolate the role of the particle size of granular materials, Wang et al. [14] conducted a series of direct shear box and triaxial tests on unbonded granular materials containing no fine. They found that the angle of internal friction φ'increased together with D_{50}, however, Cu was observed to decrease at the same time. Liu et al. [15] investigated the role of particle gradation on the strength of unbonded granular soil through Cu. They performed undrained triaxial tests where D_{50} was maintained constant. Their study suggested that the peak stress dropped as Cu increased.

A more detailed study on the influence of particle size and gradation, conducted under drained conditions, was done by [16]. They reported that D_{50} significantly influenced the behavior and the strength characteristics of granular materials, especially for a given pressure and density the rate of stress ratio was found to decrease while D_{50} increased. Furthermore, the angle of internal friction φ' was observed to decrease with the increase of D_{50}. Under low confining stress, dense sandy soil was evaluated to display a higher stress ratio. Thus, it can be observed that there is no convergent view from the aforementioned studies on the manner in which particle size and gradation of granular soils impact their engineering behavior and mechanical properties.

*Corresponding author.
Email address: ricardo@itu.edu.tr
doi: 10.14456/easr.2022.46

Taken as a whole, among the experiments conducted to study the effect of particle size and gradation on the shear strength and stress-strain of granular soils, most of them have been conducted only on unbonded soil samples. However, in natural conditions soils can be bonded, and thus behave differently [17, 18].

Several researchers have pointed out the role of bonding to improve the characteristics of soil strength and alter soil behavior [19-23]. While there is a general agreement that bonding improves soil strength and cohesion intercept, there is less agreement regarding its effect on the peak angle of internal friction φ′.

Some scholars [24, 25] identify the increase in φ′ as a result of bonding enhancement, traduced by the augmentation of the slope of the failure envelope. On the other hand, others have reported no variation in φ′ while the bonding level increases, illustrated by constancy in the slope of the failure envelope [26-28]. In fact, the first group of researchers justified the variation in φ′ as being the consequence of the interaction between the clusters and sand particles, enabling an increase in the dilatancy and strength. Others have reported that the increase in φ′ for weakly cemented soils is uncertain and, their difference from bonded to unbonded soil materials is negligible as the number of clusters from the debonding process is limited. Furthermore, the stability between the two opposite tendencies maintains the equilibrium in φ′, from which bonding reinforced the contacts between soil particles whereas the presence of fine cementing agent particles allowed more dissipation of the frictional energy. Hence, among mechanical properties, the angle of internal friction, in any case, requires more attention and needs to be further studied.

In the literature it is notable that there has rarely been any investigation into the mechanical properties of sandy soils in both bonded and unbonded states coupled with the particle size for a given fine content percentage. Nearly all previous works on the behavior of sandy soils were done on either unbonded sandy soils (with variation in fine content in most cases) or bonded sands with no variation in terms of particle size. Therefore, the research described in this article aimed to study the combined effect of bonding and particle size on the engineering behavior and mechanical characteristics of sandy materials, in which the fine content remains constant. In this regard, a series of monotonic consolidated undrained compression triaxial tests were conducted at different cell pressures, and some specific features of the mechanical behavior of the tested soils are reported.

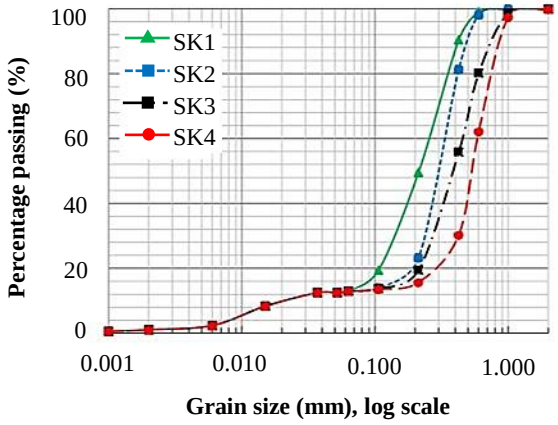

Figure 1 Grain size distribution of sand-kaolin mixtures

2. Methods and materials

2.1 Materials tested

In this experiment, artificial bonded soils were made in the laboratory by firing sand-kaolin mixture in a high-temperature furnace. The firing of sand-kaolin soil mixture in a predetermined proportion aims to simulate the properties of residual soil, weakly bonded geomaterial, as described in [29].

The sand used in the experiment is commercially clean, identified often as “Sile sand”, from North-Eastern Istanbul. The properties of kaolin and sand-kaolin used in this study are listed in Table 1. The grain size of the four sands and kaolin analyzed from the results of sieve and hydrometer analysis, respectively, are shown in Figure 1.

2.2 Sample preparation

The triaxial consolidated isotropic undrained monotonic compression (CIU) tests were conducted on both bonded and unbonded samples to obtain the shear strength parameters. The artificial bonded specimens were prepared by modifying previous research work [29].

Sand and kaolin were dry mixed in a weight ratio of 87% and 13%. It is worth pointing out that this proportion of sand and kaolin mixture was established first by [29] after an exhaustive study, as the optimum one for weakly bonded soil. It sought to simulate the behavior of residual soils. High similarities in terms of behavior were observed, after comparing artificial samples and natural residual specimens from in-situ, which encourages other studies to use this method. The sand-kaolin mixture was thoroughly mixed with distilled water. The water content was determined after a trial preparation to reach a relative density of 90% for the produced samples. Cylindrical PVC molds (a 4.4 cm diameter and 9.0 cm height) of twelves holes were utilized, in which the wet sand-kaolin mixture was carefully poured. A mold was composed of two half parts fixed with rubber bands. A mold contains in its two filter papers, one lateral and cylindrical and the other circular at the bottom, both interconnected with glue. A batch of six samples could be prepared at a time. Samples were dried in laboratory conditions for three days, after which they could stand by themselves. Bonded specimens were fired in a high-temperature furnace at 500°C for 5 hours. Once mixed with sand and water, kaolin coats and establishes bridges between the sand particles; after firing the specimen forms bonds between the sand particles. The unbonded samples were produced as the bonded ones without firing them; by doing so, there is no bonding because the presence of kaolin between sand grains establishes

contacts but without bonded bridges. Bonds result from the firing process of the dry sample, which leaves an open structure like in residual soils. Consequently, in an unfired sample, there is no bonding in terms of cementation. Thus, an unbonded sample would behave differently from a bonded one. A sample of 38 mm diameter by 76 mm high was made after carefully trimming for the CIU tests. In Appendix portrays some pictures of the sample-making process.

Table 1 Physical and Index properties of sand and kaolin

Sand (87%) - Kaolin (13%) mixture										
Material	**Grain shape***	**Gs**	**D_{10}**	**D_{50}**	**Cu**	**Cc**	**e_{max}**	**e_{min}**	**Dr**	**% FC**
Sand1 +Kaolin (SK1)	Sub-angular	2.694	0.02	0.204	12.165	3.835	1.256	0.541	0.90	13
Sand2 +Kaolin (SK2)	Sub-angular	2.691	0.02	0.287	16.280	8.018	1.220	0.531	0.90	13
Sand3 +Kaolin (SK3)	Sub-angular	2.689	0.02	0.361	21.670	7.567	1.154	0.506	0.90	13
Sand4 +Kaolin (SK4)	Sub-angular	2.686	0.02	0.508	28.495	14.856	1.150	0.488	0.90	13
Kaolin										
***LL* (%)**	***PL* (%)**	***PI* (%)**	***SL* (%)**	***LS* (%)**	**G_s**	***FC* (%)**				
62	34	28	15	5	2.61	100				

Gs = specific gravity [30], D_{10} = effective grain diameter, D_{50} = mean grain size, Cu = coefficient of uniformity, Cc =Coefficient of gradation, e_{min} = minimum void ratio index [31], e_{max} = maximum void ratio index [32], Dr = relative density, FC=Fine content, LL=liquid limit and PL=plastic limit [33], PI=plastic index. SL=shrinkage limit, LS=linear shrinkage.
*grain shape of sand material.

2.3 Experimental procedures

In the present work, CIU tests were performed to examine the combined effect of bonding and grading on the behavior of saturated weakly bonded sand. Tests were conducted under three different confining stresses of 30kPa, 200kPa, and 700kPa. The shearing phase was done at a deformation rate of 0.076 mm/min. A total of twenty-four tests were performed. The four groups of sand-kaolin soil mixtures were identified as SK1, SK2, SK3, SK4, illustrated in Figure 1. The material at bonded and unbonded states are designated by the symbol "B" and "U", respectively, which are followed by a number indicating the applied confining stress in kPa.

The CIU tests consist of three phases: saturation, consolidation, and shearing. Bonded specimens were saturated by boiling, following the procedure proposed in [29]. First, a specimen was installed on a porous stone in cold water. Then, the temperature was raised progressively over 40 minutes for the water to begin boiling. The boiling operation took a further 20 minutes. The specimen and the hot water were allowed to cool overnight. To avoid desaturation and air being trapped during test set-up, the filter papers, the second porous stone, and the membrane took place underwater. The same water was used for the whole procedure. Its transfer to the triaxial cell was carefully done. In general, this method was found to be enough to reach the targeted saturation level, but for precaution, small back pressure was applied for 3 hours and the Skempton's parameter B value of at least 0.95 was archived. For unbonded specimens, only a back-pressure method was applied to record at least 0.95 of B value. As the samples contain 87% of sand, the saturation process would take 24 hours. Both bonded and unbonded specimens were isotropically consolidated at the three aforementioned confining stresses. Consolidated time was fixed at 2 hours before the shearing phase. Thereafter, the shearing phase was applied.

Throughout the experiment, the cell pressure was maintained constant while the axial pressure was increased. The conventional triaxial testing procedures are described in detail in [34]. The excess pore pressure variation and the axial displacement were monitored by an automated pore water measurement system and a Linear Variable Differential Transducer (LVDT), respectively. A load cell of 5 KN as the maximum capacity was employed for the axial load measurement. All measurements archived accuracies beyond the requirements specified in [35].

Deviatoric stress q (Equation 1) and mean effective stress p'(Equation 2) are computed under asymmetric conditions:

$$q = \sigma_1 - \sigma_3 \tag{1}$$

$$p' = (\sigma_1' + 2\sigma_2')/3 \tag{2}$$

3. Results and discussions

Figures 2 (a)-(d) depict the stress-strain and stress path diagrams of the bonded and unbonded tested materials, respectively, gathered from this experiment. In general, the pattern of bonded soil is noticeably different from the unbonded one, especially at low strain (axial strain ε_a < 1%). At this strain, the bonded material displays a higher stiffness than the unbonded soil (Figures 2 (a) and (c)). This observation is independent of the confining pressure (σ_3) level and the mean particle size of the tested specimens. Moreover, at σ_3=30kPa and 200kPa bonded samples display an apparent peak deviatoric stress (q_p) associated with the failure, which occurs at ε_a < 2% in contrast to the responses of the unbonded samples as shown in Table 2. In fact, in a lower applied confining pressure the soil sample is less restrained due to the limited applied normal stress in the failure plane. Consequently, the subjected stress is transmitted from a block of sand particles to one another, enabled by bonding, in which the bonds play an important role. Then, once the second yield is reached, a point of major damage in terms of bonds, near the peak strength, a sudden loss of strength takes place. The latter results from a destructuration of sand particles and the limited force from the boundaries, which results in a brittle response. Besides, after being fired, kaolin establishes a connection between sand particles enabling bonded materials to sustain higher stress. As the stress increases, an important part of the bond is broken after reaching the maximum stress ratio $(q/p')_{max}$. As a consequence, after the maximum strength is reached the bonded material behaves more frictionally and its response becomes similar to the destructured samples [18, 36]. Furthermore, after the peak strength is reached (at $(q/p')_{max}$) at high strain, the force-chain buckles the bond structure leading to the apparition of shear banding [24].

Alongside the stress-strain curves, the corresponding effective stress graphs are plotted in the (q, p') plane in Figures 2 (b) and (d). From these figures, the variation of the mean particle size of the sand grains does not significantly affect the stress path in both states. However, a noticeable difference is observed in Figures 3 (a)-(c), in which the stress ratio (q/p') is plotted against axial strain at various confining pressures.

Table 2 Axial strain evolution and brittleness index (I_B) results

Test remark	State	σ_3 (kPa)	D_{50} (mm)	Axial strain (%)		I_B
				At q_{max}	At $(q/p')_{max}$	
SK1_U30	Unbonded	30	0.204	16.00	15.88	0.00
SK1_U200	Unbonded	200	0.204	18.20	15.74	0.01
SK1_U700	Unbonded	700	0.204	14.00	12.11	0.01
SK1_B30	Bonded	30	0.204	0.84	0.73	0.32
SK1_B200	Bonded	200	0.204	1.44	1.38	0.32
SK1_B700	Bonded	700	0.204	13.15	10.27	0.20
SK2_U30	Unbonded	30	0.287	19.65	12.54	0.01
SK2_U200	Unbonded	200	0.287	18.19	11.70	0.01
SK2_U700	Unbonded	700	0.287	16.67	13.53	0.02
SK2_B30	Bonded	30	0.287	1.84	1.42	0.23
SK2_B200	Bonded	200	0.287	0.96	0.96	0.23
SK2_B700	Bonded	700	0.287	10.35	8.88	0.07
SK3_U30	Unbonded	30	0.361	24.11	22.77	0.15
SK3_U200	Unbonded	200	0.361	15.52	13.64	0.03
SK3_U700	Unbonded	700	0.361	12.45	11.48	0.12
SK3_B30	Bonded	30	0.361	1.00	0.74	0.44
SK3_B200	Bonded	200	0.361	1.21	1.09	0.34
SK3_B700	Bonded	700	0.361	10.78	9.20	0.17
SK4_U30	Unbonded	30	0.508	23.33	15.46	0.07
SK4_U200	Unbonded	200	0.508	24.17	14.55	0.01
SK4_U700	Unbonded	700	0.508	16.67	9.20	0.01
SK4_B30	Bonded	30	0.508	2.06	1.35	0.44
SK4_B200	Bonded	200	0.508	1.53	1.46	0.09
SK4_B700	Bonded	700	0.508	11.94	10.24	0.06

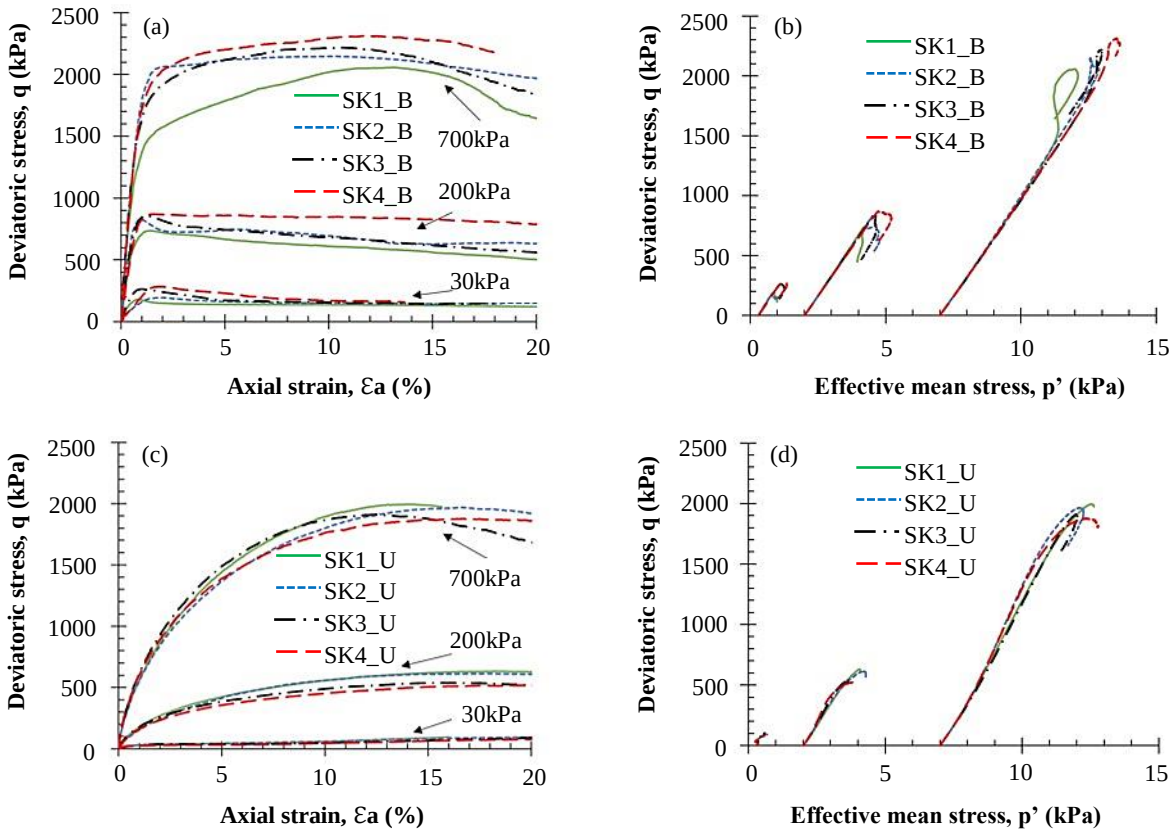

Figure 2 Strength characteristic curves of: bonded samples (a) stress-strain (b) stress-mean effective stress, unbonded specimens (c) stress-strain (d) stress-mean effective stress

3.1 Influence of the mean particle size on the stress ratio (q/p')

Figures 3 (a)-(c) show the variation of the stress ratio as a function of axial strain at 30kPa, 200kPa, and 700kPa confining pressures. In general, it is observed that for bonded specimens $(q/p')_{max}$ and D_{50} increase together. However, the tendency is reversed for unbonded materials, especially under 200kPa and 700kPa. This behavior is due to the inter-particle connection. The confining pressure plays an important role, from σ_3 =30kPa to 700kPa the bonded soils display strain-softening and strain-hardening responses,

respectively. At the high cell pressure, 700kPa, all bonded soils do not present a peak deviatoric stress and a similarity in the response can be found with the paths of the unbonded specimens. An interesting observation is that the lower confining pressure enables bonds to be broken down later after reaching $(q/p')_{max}$, while for higher stress levels, the bonds are destroyed earlier, allowing the soil to display a frictional dominant response. This behavior was also observed for bonded sands by other researchers [21, 37, 38]. The change of the shear strain in the specimen contributes to the formation and failure of interparticle connection, which is related to the particle size. In specimens of larger D_{50}, the interparticle contacts are governed by bigger particle pairs, which leave important voids between particles and generate diffuse webs of load-bearing particles [16, 39]. In the bonded state kaolin fills those pores and makes important bonding connections, this enhances the stress-bearing capacity of the soil of larger D_{50} than the smaller one, since the bonding process permits sand grains to form a block. However, in an unbonded state, this condition is omitted, particularly under saturation conditions where all kaolin contacts are disintegrated. As a result, any big web appears as a point of weakness, hence their sum-up providing a loss in strength.

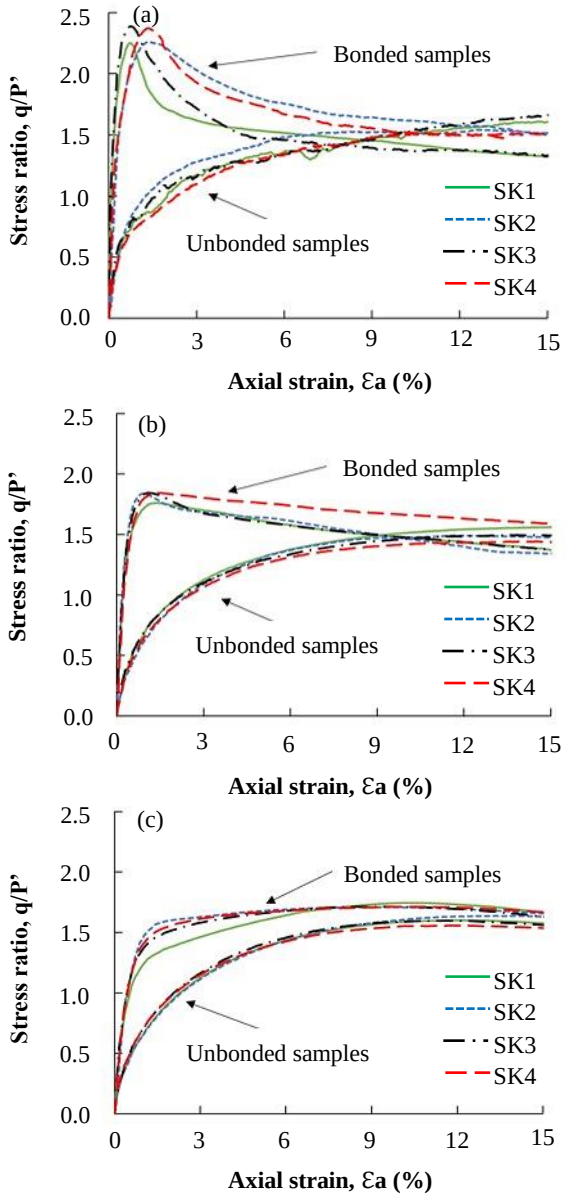

Figure 3 Stress ratio variation with strain at (a) σ_3=30kPa (b) σ_3=200kPa (c) σ_3=700kPa

3.2 The combined effect of grading characteristics and bonding on the peak strength

3.2.1 The mean particle size D_{50} and bonding

From Figures 4 (a)-(c), there is an obvious enhancement of the peak strength due to the increment of D_{50} for the bonded soils. For instance, at σ_3=30kPa the peak deviatoric stress increases from 179.74kPa to 281.98kPa, respectively, for D_{50}=0.2038mm (SK1) and 0.5084mm (SK4). The trend is even more pronounced at σ_3=700kPa, illustrated by the variation of the slope "A" of the equation. The constant A comes from the relationship between q_p and D_{50} expressed in terms of linear regression as $q_p = A * D_{50} + B$ at a given confining stress. These equations are shown in Figure 4 (a)-(c). This evolution can be explained by the strong inter-particle forces of the sample of higher D_{50} (e.g., 0.5084mm-SK4) which leads to a higher resultant normal force. For the same amount of kaolin fired, a bigger size particle offers a large surface contact, which once the kaolin is fired and the bonds established results in a stronger inter-particle connection and consequently strengthens samples of the bigger mean particle size D_{50} more effectively.

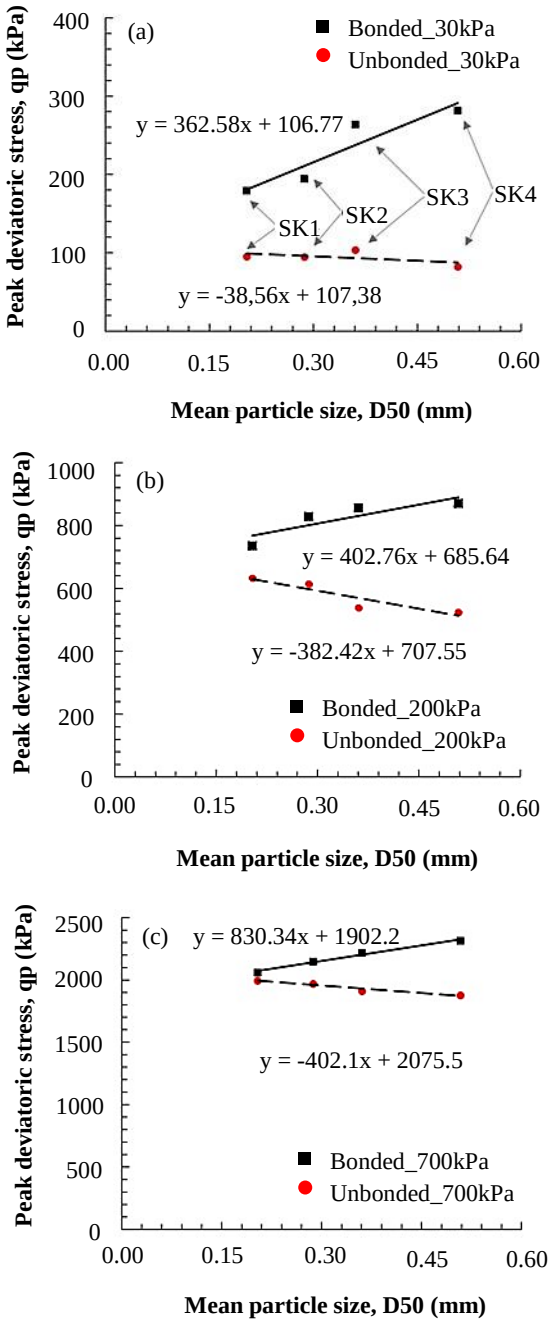

Figure 4 Variation of peak strength against mean particle size at (a) σ_3=30kPa (b) σ_3=200kPa (c) σ_3=700kPa

When comparing the results of the tests conducted on the bonded samples to the ones done on the unbonded tested specimens, the opposite pattern is observed but with a smaller rate, especially at low confining pressure (30 kPa). Figure 4 enables the authors to state that the decrease in the peak strength is slightly smaller (A= -38.56). For the unbonded specimens, only the frictional strength component is taken into account, and as the tested samples are densely packed, the unbonded soil of smaller D_{50} shows more pronounced stress [16]. During the shearing phase, especially at low strain, the particle of larger diameter size from the unbonded soil, having no or negligible cohesion, tends to rotate more easily than the smaller one, which results in an effective diminution of strength. This phenomenon is more apparent as the confining stress increases, allowing the soil to be subjected to higher stress. Even though bonding is known to play a remarkable role in low confining stress, its combination with the increment of D_{50} shows that, even at higher stress, it may consequently impact the soil strength of a larger average diameter. The authors observe that, for smaller D_{50} values in both bonded and unbonded states, the peak undrained strength at a specific confining pressure converges towards the same values.

The ratio of strength in both bonded and unbonded states with respect to D_{50} is outlined in Figure 5. The effect of bonding on D_{50} is evident. This effect is more significant at low stress with the slope "A" of the linear regression line increasing from 1.64 to 5.21, respectively, between σ_3=700kPa and 30kPa. The "A" values can be consulted from Figure 5.

Equation (3) establishes the relationship between the strength, the mean particle size, and the confining stress in bonded and unbonded states. This equation was made based on the bilateral regression relationship between these four parameters: bonded strength q_b, unbonded strength q_u, mean particle size D_{50}, and confining pressure σ_3.

$$q_b/q_u = ln\left(\sigma_3{}^{(-1.1D_{50}+0.063)}\right) + 7.91D_{50} + 0.51 \quad (3)$$

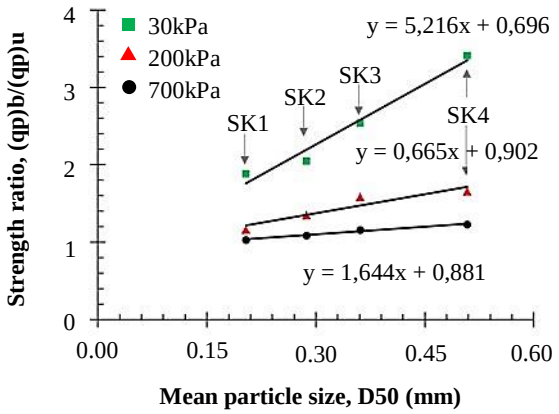

Figure 5 Bonded and unbonded stress ratio versus mean particle size

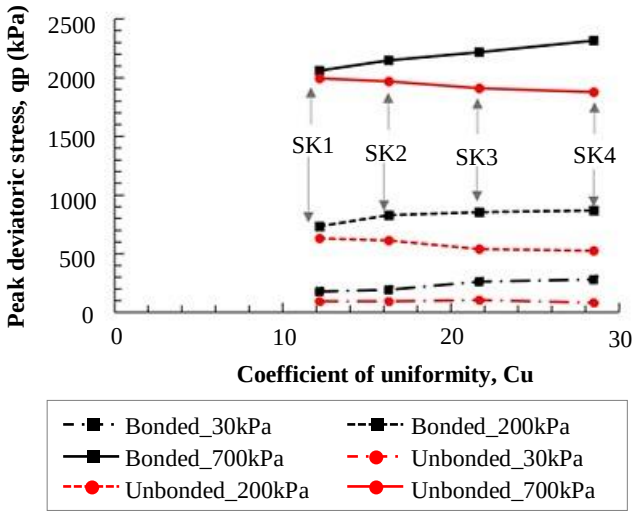

Figure 6 Variation of peak deviatoric stress with the coefficient of uniformity under different confining pressures at bonded and unbonded states

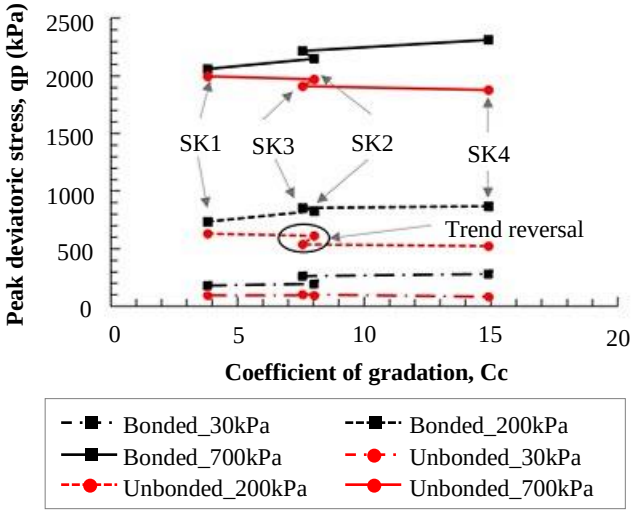

Figure 7 Variation of peak deviatoric stress with the coefficient of gradation under different confining pressures at bonded and unbonded states

3.2.2 The coefficient of uniformity Cu and bonding

Figure 6 shows the variation of the peak undrained strength with Cu for both bonded and unbonded soils. From this figure, it is observed that D_{50} and q_p increase together for tests performed on the bonded soils, however q_p decreases when D_{50} increases for the unbonded samples. Independently from the mean particle size D_{50}, the peak strength q_p and the confining pressure σ_3 vary in the same direction. These observations are linked to those made in the previous section, which were explained in detail. Thus, from the current study, there is a similarity in the D_{50} and Cu evolution, so only D_{50} is set as a reference variable.

3.2.3 The coefficient of gradation Cc

The variation of the peak strength q_p with the coefficient of gradation Cc and bonding is depicted in Figure 7, in which contrary to D_{50} and Cu, Cc does not increase and decrease straightly with q_p in bonded and unbonded states, respectively. Indeed, the value of Cc for SK2 (8.02) is higher than the one from SK3 (7.57), which does not follow the normal tendency, thus allowing the authors to notice that Cc should not be used as a reference parameter when studying the effect of material gradation. This is in agreement with the observation reported by other researchers such as in [12], who pointed out that Cc is not an appropriate parameter when evaluating the properties of soil concerning its gradation.

3.2.4 The cohesion and angle of internal friction

The cohesion intercept (c') and the angle of internal friction (φ') are among the main engineering strength properties of soil. The variation of these properties may significantly modify the strength and stability of the soil, which could lead to failure. The two parameters were calculated based on data gathered from the peak state of the CIU tests. The addition or presence of cementation in soil improves its properties by enabling the treated soil to sustain higher stress due to the gain in c' and φ'.

A close evaluation of the bonding effect on the four types of geomaterial studied indicates a net increase of φ' due to the presence of bonding (Figure 8). This gain is more remarkable for samples of the biggest D_{50}. In the latter case, the corresponding φ' increases from 37.05° to 40.41° for unbonded and bonded materials, respectively. For the unfired samples the effect of D_{50} on φ' is relatively higher compared to one of the bonded materials. The bonded samples show a tiny drop-in φ' while D_{50} gets bigger, which can be illustrated by $\varphi' = 40.96°$ for SK1 and turns to 40.41° for SK4. However, under unbonded state φ' drops more significantly when D_{50} increases, with a loss of around 2°. It is noted that the absence of bonding results in a diminution of φ', and this loss is estimated to be at least twice the one from the bonded materials. Lambe and Witmann [40] reported that the frictional angle depends on the inter-locking conditions between the grains of soils, which are related to many components such as the normal stress, soil packing density, grain shape, soil gradation, etc. In the range of D_{50} used in the present study, bonding seems to have a more predominant role on φ' than the variation of grading.

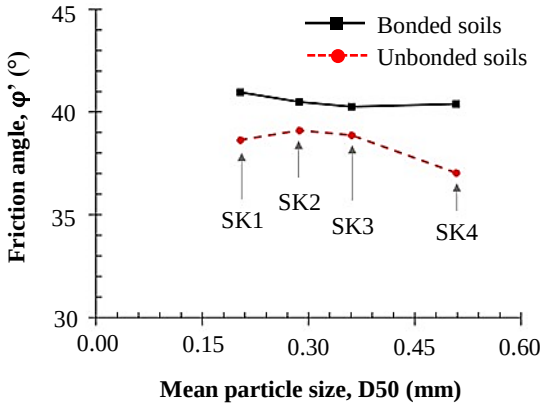

Figure 8 Variation of the angle of internal friction as a function of mean particle size for bonded and unbonded samples

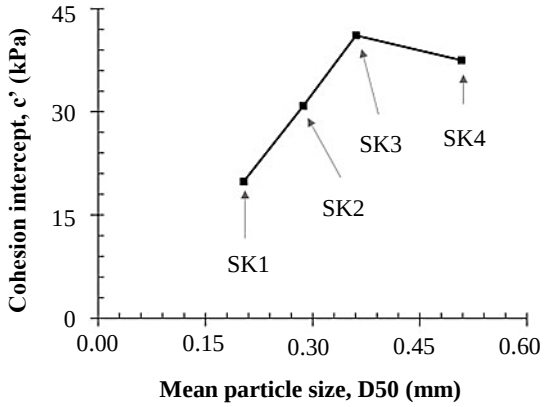

Figure 9 Variation of cohesion intercept of bonded samples as a function of mean particle size

Figure 9 depicts the variation c' in terms of mean particle size D_{50} for bonded specimens. The unbonded materials do not display a cohesion intercept. The kaolin provided none or negligible cohesion intercept. Indeed, once the unbonded soil sample is saturated, all the contacts established by the presence of kaolin between sand particles are broken up. If no boundaries are applied, such as confining pressure in the CIU test, the sample will be disintegrated. For this reason, saturated unbonded samples could not be performed in tests such as the unconfined compression test. The bonded maximum value of c' is 41.10kPa corresponding to SK3, D_{50}= 0.361mm. The cohesion intercept c' is observed to vary with two tendencies, an important augmentation from SK1(19.88kPa) to SK3(41.10kPa), followed by a slight diminution at SK4(37.49kPa). The decline in c', from SK3 to SK4, can result from a relative insufficient amount

of kaolin used for SK4 mixture, which would not coat all of the optimum specific surface of big sand particles; this would be an interesting topic where the percentage of kaolin may vary while keeping the same range of the sand mean size particle; however, this is beyond the scope of the present study. The development of c' in bonded samples is due to the enhanced connections created by the fired kaolin between the soil particles. An interesting observation is that under the same bonding condition the soil of bigger D_{50} gains more c' than the smaller one. This finding could be significant, especially for the design of the earth retaining structures and the foundation of structures built on residual soils, in which the cohesion intercept has an important role to play for its stability.

3.2.5 Brittleness index I_B

The brittleness index, I_B, expresses the loss of strength after archiving the peak deviatoric stress, q_p, as specified in [41], and illustrated by Equation (4) as

$$I_B = (q_p - q_r)/q_p \quad (4)$$

Where q_r is the residual deviatoric stress after the initial peak. In the current study q_r was considered at $\varepsilon_a = 20\%$ or at the end of the test, whichever comes first. I_B varies from 0 to 1. $I_B = 1$ indicates complete brittle response, while $I_B = 0$ is a synonym of total ductile behavior.

The evaluation of I_B was performed based on the stress-strain pattern of the materials illustrated in Figures 2 (a) and (c). The tested artificial soils displayed I_B values ranging between 0.00 and 0.44, representing the expansion characteristic of the undrained response of the bonded and unbonded materials. However, a divergent tendency was observed between the bonded and the unbonded samples. The bonded specimens are found to be more brittle with I_B ranging from 0.06 to 0.44, whereas the unbonded samples displayed I_B values less than 0.07 except for SK3_U where I_B=0.15 (Figure 10). Maccarini [29] reported the same observation when comparing bonded and unbonded soils.

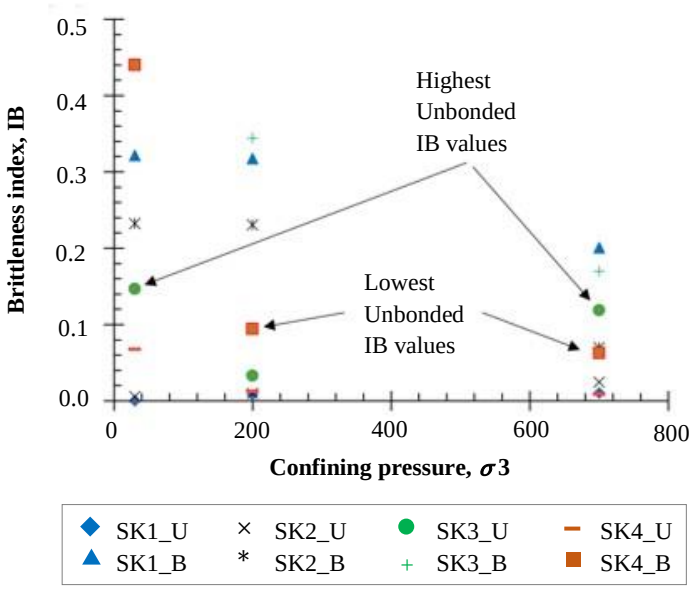

Figure 10 Variation of brittleness index with confining stress of bonded and unbonded specimens

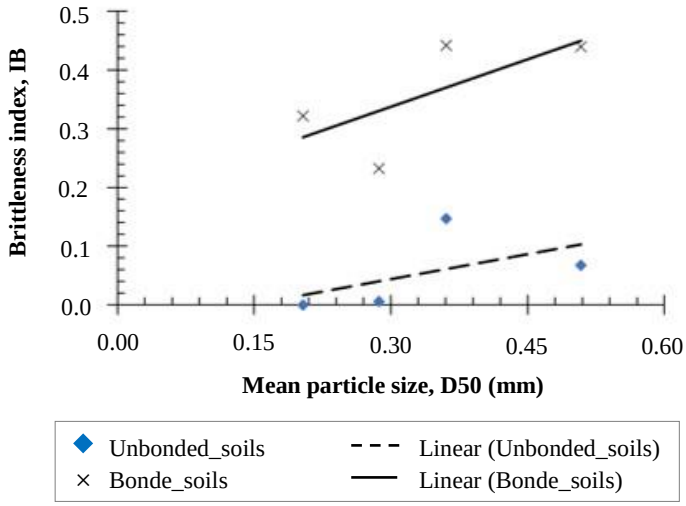

Figure 11 Variation of brittleness index with the mean particle size of bonded and unbonded soils

Furthermore, we notice that there is a common trend, from the results gathered in the experiment, which is that at low cell pressure stress (30kPa), bonded soils are highly brittle (Table 2). This observation is also seen from Figure 10, where the highest point is localized at the lowest stress σ_3=30 kPa. The unbonded samples, in contrast, showed a ductile tendency, expressed by a lower I_B (Table 2). The latter is due to the cohesionless characteristic of these soils. Some researchers [4, 23, 25] have presented similar test results for cemented soils, where the stress-strain behavior of structured samples changes from brittle to ductile because of the augmentation of confining stress.

Figure 11 shows the evolution of the brittleness index I_B with D_{50}, for both bonded and unbonded materials at 30kPa. In general, the rise in D_{50} results in a higher I_B, expressing the susceptibility of the soil of higher D_{50} to fail spontaneously. However, in the civil engineering field, this kind of failure is a big concern and it has to be avoided. A typical case of a sudden loss of strength is the failure of fill slopes, especially when subjected to an important tropical rainstorm, which results from an increase in excess pore water pressure implying a reduction in effective stress [42]. Thus, when an artificial cementation process has to be made one should adequately choose the physical properties of sand to be used.

4. Conclusion

Consolidated undrained tests were conducted at different confining stresses in order to study the combined effect of bonding and particle size on the behavior of sandy soil. Based on the experiment results, the following conclusions can be drawn:

- The presence of bonding significantly improves the mechanical properties of soil, and, when coupled with the increase of mean particle size, the enhancement is accentuated.
- The influence of both bonding and particle size is clearly established at low confining stress. The increase of confining pressure level strongly restrains the bonding impact. However, for unbonded soil, the effect of particle size is expressed more at a high-stress level.
- Among the various parameters whereby the contribution of particle size and gradation is evaluated, the coefficient of curvature is found to be less reliable.
- The angle of internal friction increases alongside the presence of bonding, whereas it decreases when D_{50} increases. The drop-in φ' is more pronounced for the unbonded materials but it is tiny for bonded soils. This divergence, between both states, is associated with the state of kaolin and the contact area of a single sand particle. Besides, the increment of cohesion intercept is found to be related to the presence of bonding, and it increases together with D_{50}.
- The unbonded samples were found to be more ductile, whereas the bonded specimens display a brittle response, especially at low confining pressure. Furthermore, the bonded soil of bigger mean particle size D_{50} is less ductile than the ones of smaller D_{50}.

In the present study, four soil materials were used to evaluate the combined effect of grading and bonding on the soil. However, the experiment could be expanded to a greater range of materials in terms of D_{50}, Cu and Cc, which may contribute to deepening the understanding of the combined effect of bonding and material gradation on the behavior and strength of geomaterials.

5. References

[1] Airey DW. Triaxial testing of a naturally cemented carbonate soil. J Geotech Eng. 1993;119(9):1379-98.
[2] Schnaid F, Prietto PDM, Consoli NC. Characterization of cemented sand in triaxial compression. J Geotech Geoenviron Eng. 2001;127(10):857-68.
[3] Nuntasarn R. The shear strength evaluation of unsaturated soils by triaxial testing. KKU Eng J. 2011;38(3):335-45.
[4] Mola-Abasi H, Saberian M, Semsani SN, Li J, Khajeh A. Triaxial behaviour of zeolite-cemented sand. Proc Inst Civ Eng Ground Improv. 2020;173(2):82-92.
[5] Wang L, Chu J, Wu S, Wang H. Stress-dilatancy behavior of cemented sand: comparison between bonding provided by cement and biocement. Acta Geotech. 2021;16:1441-56.
[6] Mohamad R, Dobry R. Undrained monotonic and cyclic triaxial strength of sand. J Geotech Eng. 1986;112(10):941-58.
[7] Thevanayagam S. Effect of fines and confining stress on undrained shear strength of silty sands. J Geotech Geoenviron Eng. 1998;124(6):479-91.
[8] Malandraki V, Toll D. Drained probing triaxial test on a weakly bonded artificial soil. Geotechnique. 2000;50(2):141-51.
[9] Thevanayagam S, Mohan S. Intergranular state variables and stress-strain behaviour of silty sands. Geotechnique. 2000;50(1):1-23.
[10] Karimian A, Hassanlourad M. Undrained monotonic shear behaviour of loose sand-silt soil mixture. Int J Geotech Eng. 2020;14(8):919-29.
[11] Thevanayagam S, Shenthan T, Mohan S, Liang J. Undrained fragility of clean sands, silty sands, and sandy silts. J Geotech Geoenviron Eng. 2002;128(10):849-59.
[12] Belkhatir M, Arab A, Schanz T, Missoum H, Della N. Laboratory study on the liquefaction resistance of sand-silt mixtures: effect of grading characteristics. Granul Matter. 2011;13(5):599-609.
[13] Taiba AC, Belkhatir M, Kadri A, Mahmoudi Y, Schanz T. Insight into the effect of granulometric characteristics on the static liquefaction susceptibility of silty sand soils. Geotech Geol Eng. 2016;34(1):367-82.
[14] Wang JJ, Zhang HP, Tang SC, Liang Y. Effects of particle size distribution on shear strength of accumulation soil. J Geotech Geoenviron Eng. 2013;139(11):1994-7.
[15] Liu YJ, Li G, Yin ZY, Dano C, Hicher PY, Xia XH, et al. Influence of grading on the undrained behavior of granular materials. CR Mecanique. 2014;342(2):85-95.
[16] Amirpour Harehdasht S, Karray M, Hussien MN, Chekired M. Influence of particle size and gradation on the stress-dilatancy behavior of granular materials during drained triaxial compression. Int J Geomech. 2017;17(9):04017077.
[17] Vaughan PR. Characterising the mechanical properties of the in-situ residual soil. Proceedings of the Second International Conference on Geomechanics in Tropical Soils; 1998 Dec 12-14; Singapore. Rotterdam: Balkema; 1988. p. 469-87.
[18] Huang TJ, Airey WD. Effects of cement and density on artificially cemented sand. In: Anagnostopoulos A, Frank R, Kalteziotis N, Schlosser F, editors. Geotechnical Engineering of Hard Soil-Soft Rocks. Rotterdam: Balkema; 1993. p. 553-60.
[19] Clough GW, Sitar N, Bachus RC, Rad NS. Cemented sands under static loading. J Geotech Eng Div. 1981;107(6):799-817.
[20] Cuccovillo T, Coop MR. Yielding and pre-failure deformation of structured sands. Geotechnique. 1997;47(3):491-508.

[21] Cuccovillo T, Coop MR. On the mechanics of structured sands. Geotechnique. 1999;49(6):741-60.
[22] Al-Aghbari MY, Dutta RK. Effect of cement and cement by pass dust on the engineering properties of sand. Int J Geotech Eng. 2008;2(4):427-33.
[23] Porcino DD, Marciano V. Bonding degradation and stress-dilatancy response of weakly cemented sands. Geomech Geoengin. 2017;12(4):221-33.
[24] Wang YH, Leung SC. Characterization of cemented sand by experimental and numerical investigations. J Geotech Geoenviron Eng. 2008;134(7):992-1004.
[25] Marri A, Wanatowski D, Yu HS. Drained behaviour of cemented sand in high pressure triaxial compression tests. Geomech Geoengin. 2012;7(3):159-74.
[26] Kaga M, Yonekura R. Estimation of strength of silicate-grouted sand. Soils Found. 1991;31(3):43-59.
[27] Porcino D, Marciano V, Granata R. Static and dynamic properties of a lightly cemented silicate-grouted sand. Can Geotech J. 2012;49(10):1117-33.
[28] Fu Z, Chen S, Han H. Large-scale triaxial experiments on the static and dynamic behavior of an artificially cemented gravel material. Eur J Environ Civ Eng. In press 2021.
[29] Maccarini M. Laboratory studies of a weakly bonded artificial soil [thesis]. London: University of London; 1987.
[30] ASTM. ASTM D854-14, Standard test methods for specific gravity of soil solids by water pycnometer. Philadelphia: ASTM; 2014.
[31] ASTM. ASTM D4254-16, Standard test method for minimum index density and unit weight of soils and calculation of relative density. Philadelphia: ASTM; 2016.
[32] ASTM. ASTM D4253-16, Standard test method for maximum index density and unit weight of soils using a vibratory table. Philadelphia: ASTM; 2016.
[33] ASTM. ASTM D 4318-00, Standard test methods for liquid limit, plastic limit, and plasticity index of soils. Philadelphia: ASTM; 2003.
[34] Bishop AW, Henkel DJ. The measurement of soil properties in the triaxial test. 2nd ed. London: Edwin Arnold; 1957.
[35] ASTM. ASTM D4767-11, Standard test method for consolidated undrained triaxial compression test for cohesive soils. Philadelphia: ASTM; 2020.
[36] Leroueil S, Vaughan PR. The general and congruent effects of structure in natural soils and weak rocks. Geotechnique. 1990;40(3):467-88.
[37] Haeri MS, Hamidi A, Hosseini SM, Asghari E, Toll DG. Effect of cement type on the mechanical behavior of a gravely sand. Geotech Geol Eng. 2006;24(2):335-60.
[38] Ali Rahman Z, Toll DG, Gallipoli D. Critical state behaviour of weakly bonded soil in drained state. Geomech Geoengin. 2018;13(4):233-45.
[39] Oda M, Kazama H. Microstructure of shear bands and its relation to the mechanisms of dilatancy and failure of dense granular soils. Geotechnique. 1998;48(4):465-81.
[40] Lambe TW, Whitman RV. Soil mechanics. New York: John Wiley and Sons; 1969.
[41] Bishop AW. Shear strength parameters for undisturbed and remoulded soil specimens. In: Parry RH, Roscoe KH, editors. Stress-strain Behaviour of Soils: Proceedings of the Roscoe Memorial Symposium. Oxfordshire: G.T. Foulis & Co. Ltd; 1971. p. 3-58.
[42] Chen H, Lee CF, Law KT. Causative mechanisms of rainfall-induced fill slope failures. J Geotech Geoenviron Eng. 2004;130(6):593-602.

6. Appendix

Some pictures of sample preparation process: (a) kaolin, (b) two half parts of the PVC mold, (c) wet sample in the mold, (d) partially dry sample in filter paper for further drying, (e) dry sample, (f) trimmed sample, (g) furnace.

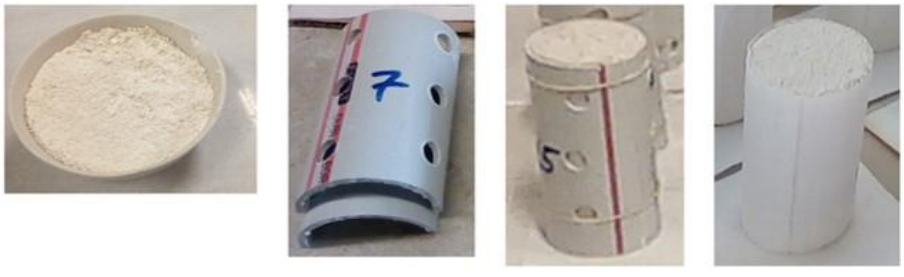

(a) (b) (c) (d)

(e) (f) (g)